Shear Wave Based Screening Method for Liquefaction Evaluation

J. Yang(✉)

Department of Civil Engineering, The University of Hong Kong, Pok Fu Lam, Hong Kong
junyang@hku.hk

Abstract. This paper describes a new screening method for evaluating the liquefaction potential of sand deposits with varying percentages of fines. The method is based on measurements of shear wave velocity (V_s), and is developed from a comprehensive experimental program comprising small-strain shear wave testing and large-strain undrained shear tests for sand samples with different quantities of non-plastic fines. A novel point of the method is the unified characterization of shear wave velocity for both clean sand and silty sand through a state parameter that properly combines the effects of void ratio and confining stress in a sound theoretical context. As modern technology has made it more convenient and reliable to measure the shear wave velocity both in the laboratory and in the field, and since the state parameter is a rational index for characterizing various aspects of soil behavior, the proposed method is promising in a wide range of geotechnical applications.

Keywords: Liquefaction · Sands · Fines · Shear wave velocity · In situ state

1 Introduction

Soil liquefaction has been a subject of long standing interest in soil mechanics and geotechnical engineering. In the past decades, soil liquefaction has been investigated mainly in the context of earthquake loading [8, 9, 16, 17, 30], due to the significant liquefaction-related damage observed during the Niigata and Alaska earthquakes in 1964. Some aspects of soil liquefaction have been well understood, many others, however, remain confusing, controversial or mysterious. The liquefaction phenomenon widely observed in laboratory undrained cyclic triaxial tests [8, 14] is characterized by repeated loss and regain of stiffness along with the development of excessive deformation. This behavior, arguably, should not be referred to as liquefaction but, more appropriately, be called cyclic mobility [4, 5]. Based on a comprehensive experimental program, Yang and his co-workers have found that undrained cyclic behavior of sand is much more complicated than previously thought and can be categorized into five major types: flow-type failure, cyclic mobility, plastic strain accumulation, limited flow followed by cyclic mobility, and limited flow followed by strain accumulation [15, 19, 26, 27]. The question as to which pattern will occur depends on a number of inter-related factors, including packing density, effective confining stress, soil fabric, initial static shear stress level and cyclic load level.

T. Triantafyllidis (Ed.): *Recent Developments of Soil Mechanics and Geotechnics in Theory and Practice*, LNACM 91, pp. 169–182, 2020.
https://doi.org/10.1007/978-3-030-28516-6_9

Among the five deformation patterns, the flow-type failure is most critical and is characterised by abrupt, run-away deformation without any precautionary signal. This failure pattern is pertinent to sufficiently loose sand and in many ways is similar to the static or flow liquefaction phenomenon observed in monotonic triaxial tests [21, 27]. Actually, a reasonable correspondence exists between the two, as shown in Fig. 1 where the results from a monotonic test and a cyclic triaxial test on Toyoura sand at a similar post-consolidation state are plotted together. Flow liquefaction, triggered by either cyclic or monotonic loading, can produce the most catastrophic effects of all liquefaction-related phenomena and therefore is a major concern in the deign and construction of large sand structures such as earth or tailings dams and artificial islands [4, 9, 10].

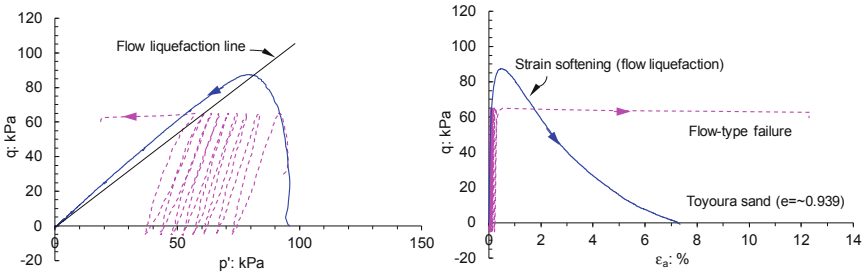

Fig. 1. Correspondence of liquefaction behavior under cyclic and monotonic loading

Whether a sand is in a loose or dense state depends not only on its density (or void ratio) but also on the effective confining stress applied. There is now a general agreement that the behavior of a sand is more closely related to the proximity of its initial state to the critical state or steady state locus [2, 21, 23], which can be described by a state parameter (ψ). If the initial state of a saturated sand lies above the critical state locus with a positive ψ value (state A in Fig. 2), it tends to contract when sheared undrained, accompanied by strain softening and a buildup of high pore water pressure. If the initial state lies below the critical state locus with a negative ψ value (state D or B), it tends to undergo a net dilation, accompanied by strain hardening to a much higher strength. The initial state defined by the void ratio and mean effective stress with reference to the critical state locus is therefore a meaningful index that can be used to identify the potential for liquefaction.

Along this line, we have developed a new method which allows a unified evaluation of *in situ* state of both clean sand and silty sand and thereafter their potential for liquefaction through shear wave velocity measurements. Theoretically, shear wave velocity is a fundamental property with clear physical meaning, directly related to the small-strain shear stiffness of soil. Practically, modern technology has advanced such that shear wave velocity can be measured more conveniently and reliably both in the laboratory and in the field [6]. This paper describes the main aspects of this promising method along with validation.

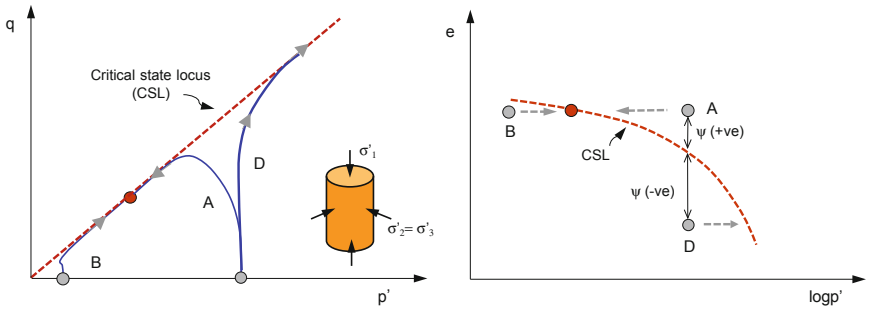

Fig. 2. Schematic illustration of state-dependent behavior of sand under undrained monotonic loading

2 Problems with Current Methods

It remains a big challenge to obtain undisturbed sand samples using conventional methods for the determination of their *in situ* state. As a result, efforts have been made to use field tests, particularly the cone penetration test (CPT), to evaluate the state of sand [1, 3]. Central to the CPT-based method is an empirical correlation between relative density (or void ratio), effective stress level and cone tip resistance, established mainly from laboratory chamber tests on clean uniform sands. Attempts have also been made to use shear wave velocity (V_s) to estimate the state of sand [13]. Similarly, the key to the V_s-based method is an empirical correlation linking void ratio, effective stress level and shear wave velocity, derived from laboratory measurements of shear wave velocity in clean sand samples. Often natural sand deposits or fills are not clean, but contain a certain amount of fines (referred to as silty sand in practice). Even within a single deposit of sand, the percentage of fines may vary appreciably. For example, the fill materials used in construction of the artificial islands in the Beaufort Sea contained non-plastic fines at percentages varying from 0 to 12%. Application of the existing CPT- or V_s-based methods implicitly requires the assumption that the empirical correlations are not affected by the presence of fines.

The assumption is, however, questionable. There is increasing evidence that for a given void ratio and confining stress, the shear wave velocity or associated shear modulus of clean sand will change with the addition of fines [20, 24]. The cone tip resistance is also known to be sensitive to the presence of fines [11, 12], which can be a cause for the considerable uncertainty with the correction factors for interpreting chamber tests. Within this context, caution should be exercised when applying the existing empirical correlations to sand deposits with fines, since they could in some circumstances cause potentially catastrophic consequences.

3 Impact of Fines on Soil Liquefaction

While it has long been recognized that the presence of fines can alter the shear behavior of sand under either monotonic or cyclic loading conditions, very diverse views exist as to whether the effect of fines is negative or beneficial for liquefaction resistance. The problem is complex due mainly to the fact that sand-fines mixtures are granular materials in nature. The characteristics of both fine and coarse particles, such as shape, size and plasticity, can affect the packing patterns and interactions of the particles and, hence, their mechanical behavior [18, 28].

Figure 3 shows a concrete example that the addition of non-plastic fines (crushed silica) to Toyoura sand can lead to a notable increase in strain softening compared with the base sand on its own at a similar void ratio. Under otherwise similar conditions, the specimen at fines content (FC) of 15% (denoted as TSS15) underwent complete liquefaction when subjected to undrained shear, whereas the clean sand specimen (TS) exhibited a strong dilative response with no liquefaction. Furthermore, Fig. 4 compares the response of a loose Toyoura sand specimen under cyclic loading with that of a loose specimen of the same sand mixed with 10% fines (TSS10) under similar testing conditions. While both specimens exhibited the flow-type behavior, the specimen TSS10 quickly failed in less than 10 cycles of loading but liquefaction of the TS specimen was not initiated until ~78 loading cycles.

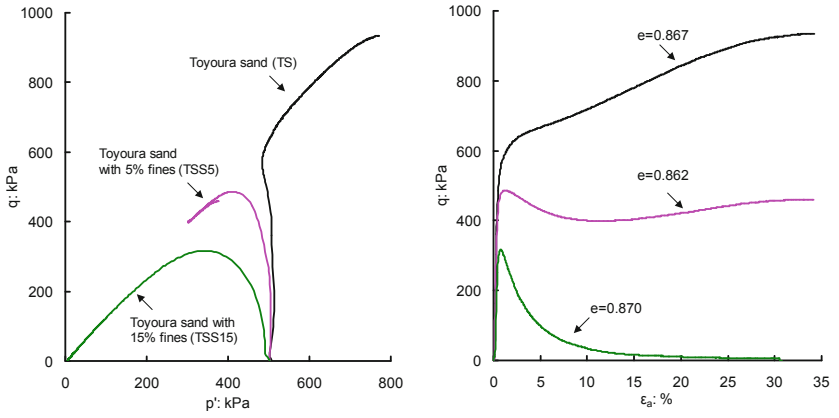

Fig. 3. Effect of fines on undrained behavior of sand under monotonic loading

It is worth noting that for both monotonic and cyclic loading tests, the effect of non-plastic fines is always an increase in liquefaction potential or a decrease in liquefaction resistance if post-consolidation void ratio is used consistently as the comparison basis. Yang et al. [29] have elaborated that the conventional global void ratio is a more rational state variable compared with such others as relative density and skeleton void ratio. Also, the fines contents concerned here are all less than a threshold value (typically ~30%) such that the sand-fines mixtures are sand dominant.

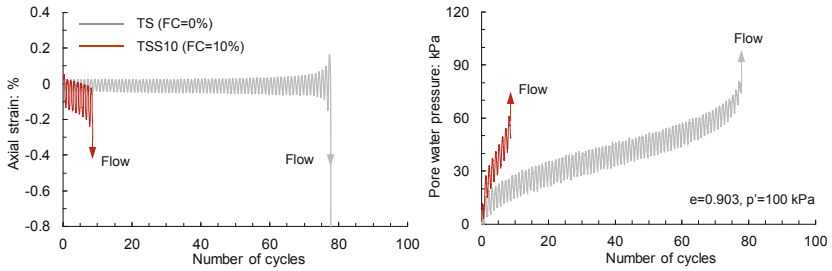

Fig. 4. Effect of fines on undrained behavior of sand under cyclic loading

4 Shear Wave Velocity Affected by Fines

A systematic investigation of state-dependent shear wave velocity in saturated sand samples with different percentages of fines has been carried out using piezoelectric bender elements. A schematic illustration of the setup for shear wave measurements is shown in Fig. 5, and more details about the apparatus and the method for data interpretation can be found in [22]. As an example, Fig. 6(a) presents a set of received signals in a TS specimen consolidated to 50 kPa, at excitation frequencies varying from 1 to 80 kHz, while Fig. 6(b) shows received signals in a TSS10 specimen at a similar state. For a given frequency, the wave form in the TS specimen appears to be similar to that in the TSS10 specimen; a careful inspection of the wave forms indicates, however, that the travel times of shear waves differ. To better view this difference, Fig. 7 shows shear wave signals recorded in four specimens (TS, TSS10, TSS20, TSS30) at the excitation frequency of 10 kHz; all the four specimens were at a similar consolidation state. It is immediately evident that the presence of a small amount of fines can lead to a notable delay in the arrival time of shear wave and, thereafter, a reduction of shear wave velocity.

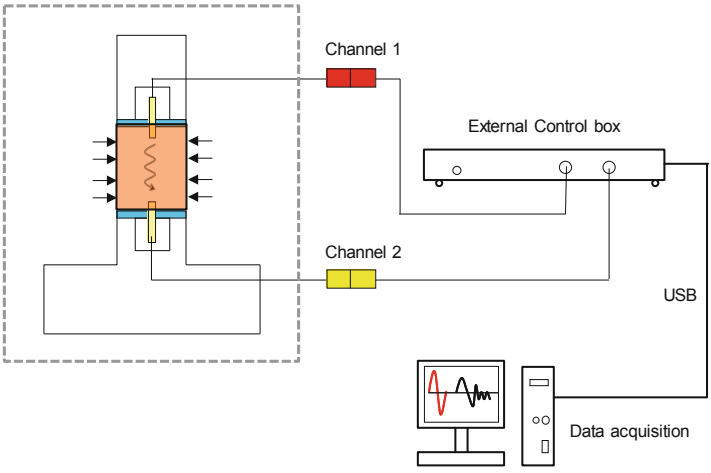

Fig. 5. Schematic illustration of laboratory setup for shear wave measurement

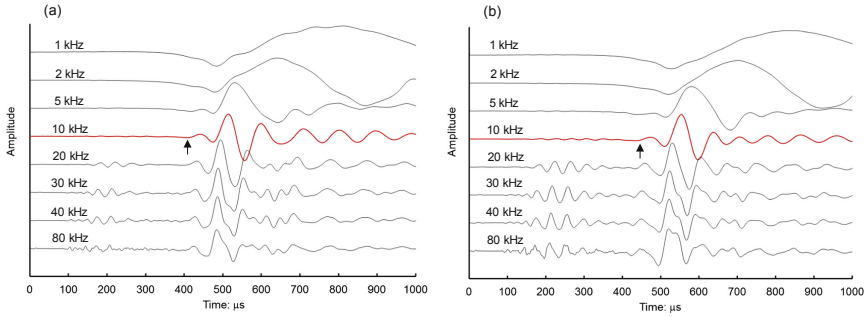

Fig. 6. Shear wave signals at various excitation frequencies for a given state (p′ = 50 kPa, e = ~0.802): (a) TS specimen; (b) TSS10 specimen

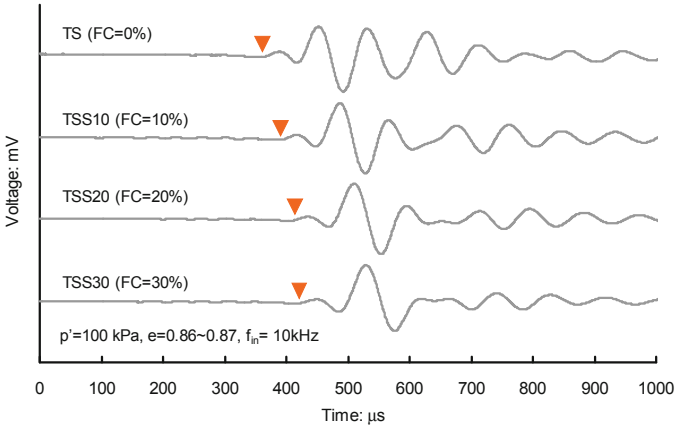

Fig. 7. Shear wave signals in saturated sand specimens with different percentages of fines

4.1 Void Ratio-Dependent Shear Wave Velocity

Measured V_s values for saturated sand specimens with different percentages of fines (TS, TSS5, TSS10 and TSS20) are plotted as a function of void ratio for two stress levels in Fig. 8. Clearly, in addition to the void ratio, V_s is also dependent on confining stress and fines content. The state dependence of V_s is often described using the following relationship [7, 13]:

$$V_s = (b_1 - b_2 e)\left(\frac{p'}{p_a}\right)^{1/4} \quad (1)$$

where p_a is a reference pressure, typically taken as the atmospheric pressure. Notice that parameters b_1 and b_2 will vary with fines content. By introducing a stress-corrected shear wave velocity (V_{s1}), a linear relationship between V_{s1} and e can readily be established as:

$$V_{s1} = V_s \left(\frac{p_a}{p'}\right)^{1/4} = (b_1 - b_2 e) \tag{2}$$

The above relationship is commonly used in geotechnical engineering practice. When all measured V_s values are corrected for stress and then plotted against void ratio, as shown in Fig. 9, one can see that this linear relationship fails to work in an acceptable way although a general trend exists that V_{s1} decreases with increasing void ratio.

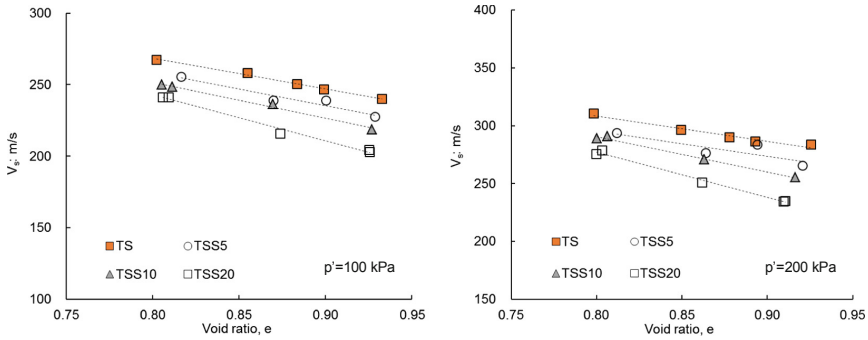

Fig. 8. Shear wave velocity versus void ratio at two stress levels

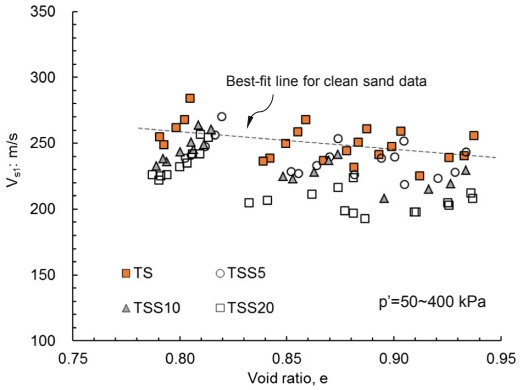

Fig. 9. Stress-corrected shear wave velocity versus void ratio

4.2 State Parameter-Dependent Shear Wave Velocity

All of the shear wave tests were conducted on saturated specimens and covered a wide range of states in terms of void ratio and effective confining stress [24, 25]. As an example, the two plots of Fig. 10 show the states of TS and TSS10 specimens with reference to their critical state loci in the e-lop' space, respectively. Note that the critical state locus moves downward with increasing fines content [28]. By calculating state

parameters, measured V_s values for clean and mixed sand specimens (TS, TSS5, TSS10, TSS20) are shown as a function of ψ in Fig. 11 at two stress levels. A striking finding is that for either stress level, all data points fall on a single straight line, regardless of fines content. This finding is significantly different from the observation in Fig. 8, obtained from the traditional method of analysis. Furthermore, using the concept of stress-corrected shear wave velocity, a unique relationship can be established between V_{s1} and ψ, which works well for all data, as shown in Fig. 12. The relationship is a simple, linear function:

$$V_{s1} = V_s\left(\frac{p_a}{p'}\right)^n = A - B\psi \tag{3}$$

where A, B and n are material constants independent of fines content. From the test results they are determined as 237.2 m/s, 281.2 m/s, and 0.222, respectively. Note that if a default value of 0.25 is assigned to n, the performance of the above relationship remains reasonably good (see the right plot of Fig. 12).

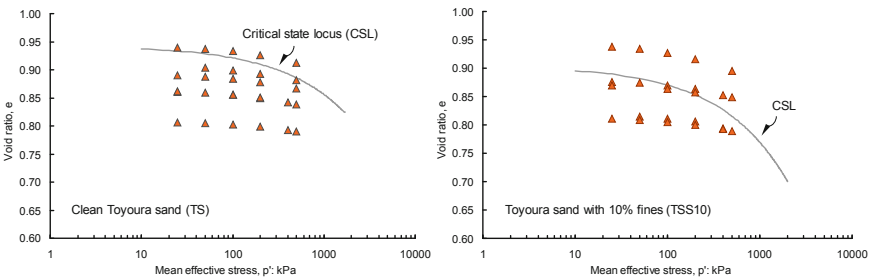

Fig. 10. States of TS and TSS10 specimens with reference to their critical state loci

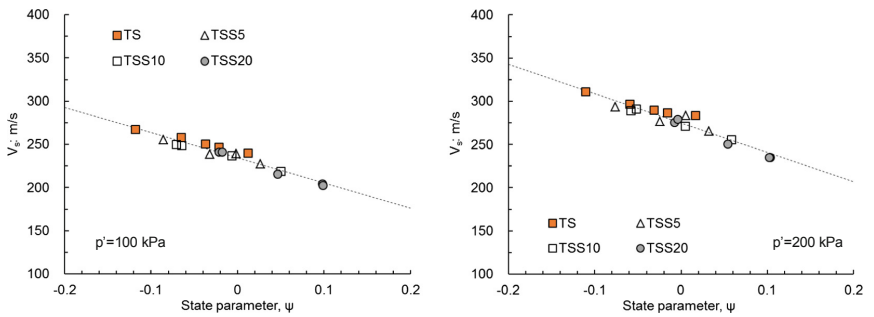

Fig. 11. Shear wave velocity versus state parameter at two stress levels

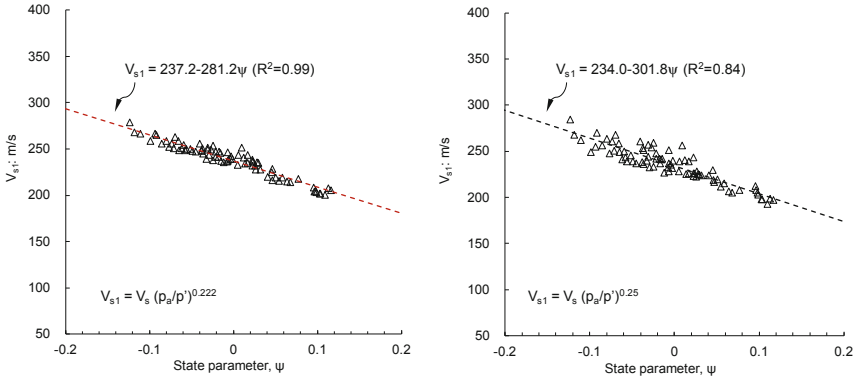

Fig. 12. Stress-corrected shear wave velocity versus state parameter for all test data

5 Evaluation of In Situ State

Freshly deposited sands are generally under normally consolidated, anisotropic conditions. The mean effective stress p' at a given depth can be estimated as

$$p' = \left(\frac{1+2K_0}{3}\right)\sigma'_v \tag{4}$$

where σ'_v is effective vertical stress at the depth and K_0 is the coefficient of earth pressure at rest. Combining Eq. (4) with Eq. (3) gives rise to an alternative form for state-dependent V_s as follows

$$V_s = (A - B\psi)\left(\frac{\sigma'_v}{p_a}\right)^n \left(\frac{1+2K_0}{3}\right)^n \tag{5}$$

Note that values of K_0 for normally consolidated, loose and medium dense sands typically vary between 0.4 and 0.6.

Using the above relationship, a set of state profiles for the sand-fines mixtures tested can be constructed in the plane of V_s and σ'_v, as shown in Fig. 13. The two plots here correspond respectively to two different K_0 values (0.4 and 1), and in each plot the set of curves represent sand states varying from $\psi = -0.2$ (highly dilative) to $\psi = +0.2$ (highly contractive). Particularly, the curve for $\psi = 0$ can be used to approximately define the boundary between a dilative-response zone and a contractive-response zone. If sand state lies in the contractive zone, caution should be exercised that the sand has a potential for liquefaction when subjected to undrained shear.

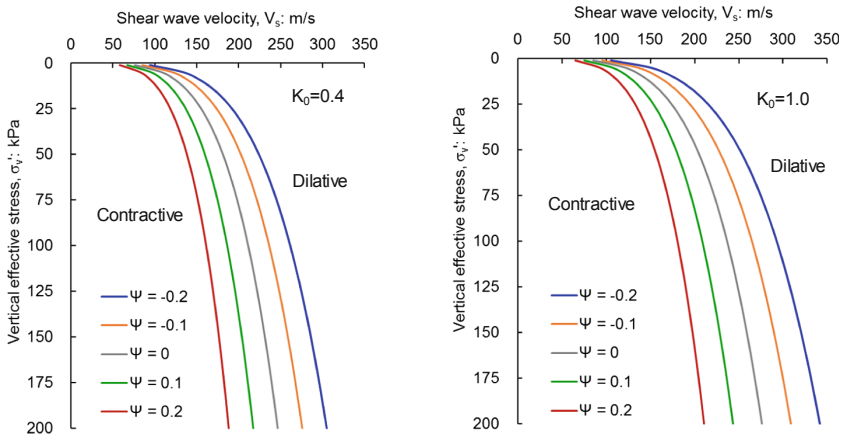

Fig. 13. State profiles in V_s–σ'_v plane at two different K_0 values

6 Validation Using Independent Tests

The significance of Eq. (3) or (5) is that it provides a unified relationship linking V_s and ψ for both clean sand and silty sand. To validate this relationship, two independent specimens were prepared: one composed of clean Toyoura sand only (TS) and the other composed of 90% Toyoura sand and 10% fines (TSS10). The TS specimen was saturated and then isotropically consolidated to the state of $e = 0.846$ and $p' = 100$ kPa, whereas the TSS10 specimen was consolidated to the state of $e = 0.904$, $p' = 300$ kPa. For both specimens, their shear wave velocities were measured using the piezoelectric bender elements. Figure 14 shows received signals at the excitation frequency of 10 kHz. The measured V_s values for the TS and TSS10 specimens are 257.5 m/s and 281.2 m/s, respectively. Provided similar mineral composition, one often makes a direct comparison of V_s measurements and concludes that the TSS specimen with higher V_s is at a denser state and hence is less susceptible to liquefaction. However, the conclusion derived from this practice is misleading.

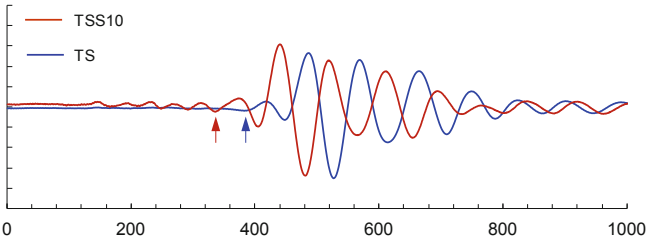

Fig. 14. Shear wave signals in two independent specimens at excitation frequency of 10 kHz

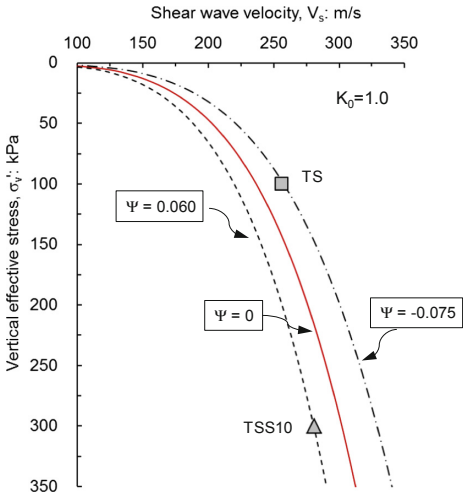

Fig. 15. Predicted state profiles in $V_s - \sigma'_v$ plane along with measured data

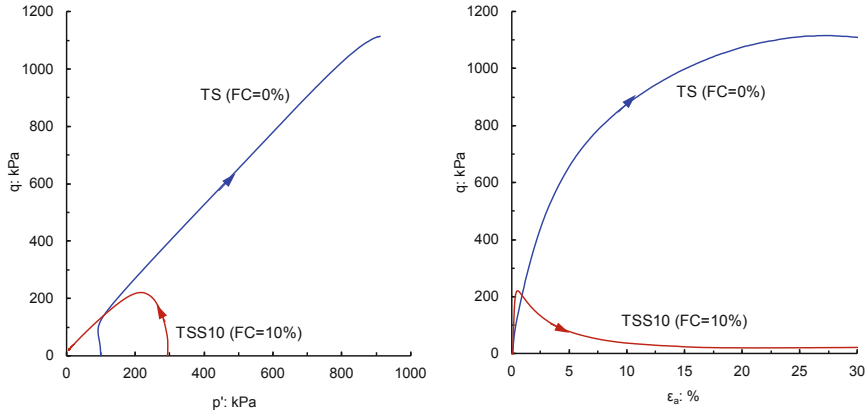

Fig. 16. Undrained shear responses of two independent specimens

The measured V_s values are plotted on the plane of V_s versus σ'_v in Fig. 15, where a set of state profiles are also given using the relationship in Eq. (5). It is noted that the TS specimen lies on the state profile for $\psi = -0.075$ while the TSS10 specimen lies on the profile of $\psi = +0.060$. As the TSS specimen lies far left of the state boundary ($\psi = 0$), one can predict that it is susceptible to liquefaction when subjected to undrained shear. On the other hand, the TS specimen lying to the right of the boundary is expected to dilate when loaded undrained.

To verify the prediction, undrained triaxial tests were conducted on the two specimens. Figure 16 shows the stress-strain curves and stress paths, and Fig. 17 compares the responses of pore water pressures. It is highly encouraging that the TSS specimen, as predicted, underwent almost complete liquefaction, with an extremely low

strength at the critical state, whereas the TS specimen exhibited a highly dilative response, achieving a large strength at the critical state.

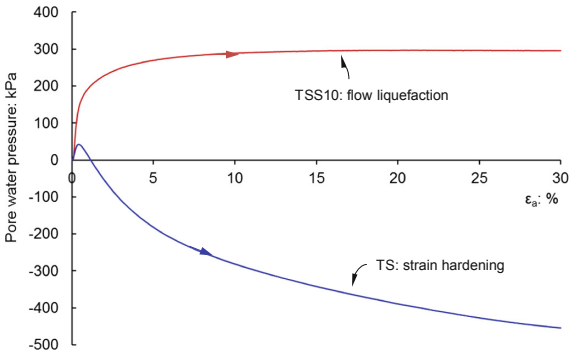

Fig. 17. Responses of pore water pressures recorded in two independent specimens

7 Conclusions

Evaluating the *in situ* state of a sand deposit and its potential for liquefaction is a challenging problem. A new method to address this problem based on shear wave velocity measurements has been described in this paper. The significant advantage of the method is that it accounts for the complicated effect of fines in a unified manner in the critical state context. Central to the method is a unique relationship established between V_{s1} and ψ that is independent of fines content. Compared with the cone penetration resistance widely used in current geotechnical applications, shear wave velocity is a basic soil property with clear physical meaning, and can be measured in soils that are hard to penetrate with the penetrometer or at sites where borings may not be permitted. Furthermore, modern technology has advanced such that shear wave velocity can be measured more conveniently and reliably both in the laboratory (e.g. piezoelectric bender elements) and in the field (e.g. SASW and seismic CPT). All these advantages make the new method appealing to a variety of geotechnical applications.

Further studies to refine the method based on laboratory and field tests on different sands with different grain characteristics are worthwhile. Also, it is necessary to mention that the method is mainly applicable to fresh, unaged sand deposits or fills. To what extent it is applicable to aged or cemented sand deposits is yet unclear; future research along the proposed line to explore this issue would be of interest. Nevertheless, it is important to bear in mind that it is the fresh, unaged sand deposits that are susceptible to liquefaction and excessive deformation.

Acknowledgments. This work is part of long-term research on soil liquefaction and related phenomena from multi-scale perspectives at The University of Hong Kong (HKU). The author is grateful for the financial support provided by the Research Grants Council of Hong Kong (Nos. 17206418; 17250316; 719105), the National Science Foundation of China (No. 51428901), the Seed Fund for Basic Research of HKU, and the Strategic Research Development Fund of the Department of Civil Engineering over the years.

References

1. Baldi, G., Bellotti, R., Chionna, V., Jamiolkowski, M., Pasqualini, E.: Design parameters for sands from CPT. In: Proceedings of 2nd European Symposium on Penetration Testing, Amsterdam, Holland, pp. 425–432 (1982)
2. Been, K., Jefferies, M.G.: A state parameter for sands. Géotechnique **35**(2), 99–102 (1985)
3. Been, K., Crooks, J.H.A., Becker, D.E., Jefferies, M.G.: The cone penetration test in sands. Part 1: state parameter interpretation. Géotechnique **36**(2), 239–249 (1986)
4. Casagrande, A.: Liquefaction and cyclic deformation of sands, a critical review. In: Proceedings of 5th Pan-American Conference on Soil Mechanics Foundation Engineering, Buenos Aires, vol. 5, pp. 79–133 (1975)
5. Castro, G.: Liquefaction and cyclic mobility of saturated sands. J. Geotech. Eng. Div. ASCE **101**(GT6), 551–569 (1975)
6. Clayton, C.R.I.: Stiffness at small-strain: research and practice. Géotechnique **61**(1), 5–38 (2011)
7. Hardin, B.O., Richart, F.E.: Elastic wave velocities in granular soils. J. Soil Mech. Found. Div. ASCE **89**(SM1), 39–56 (1963)
8. Idriss, I.M., Boulanger, R.W.: Soil liquefaction during earthquakes. EERI Monograph (2006)
9. Ishihara, K.: Liquefaction and flow failure during earthquakes. Géotechnique **43**(3), 351–451 (1993)
10. Jamiolkowski, M.: Soil mechanics and the observational method: challenges at the Zelazny Most copper tailings disposal facility. Géotechnique **64**(8), 590–619 (2014)
11. Lunne, T., Robertson, P.K., Powell, J.J.M.: Cone Penetration Testing in Geotechnical Practice. Blackie Academic & Professional (Chapman & Hall), Glasgow (1997)
12. Mayne, P.W.: Cone penetration testing. NCHRP Synthesis 368, Transportation Research Board, Washington, D.C. (2007)
13. Robertson, P.K., Sasitharan, S., Cunning, J.C., Sego, D.C.: Shear wave velocity to evaluate flow liquefaction. J. Geotech. Eng. ASCE **121**(3), 262–273 (1995)
14. Seed, H.B., Lee, K.L.: Liquefaction of saturated sands during cyclic loading. J. Soil Mech. Found. Div. ASCE **92**(SM6), 105–134 (1996)
15. Sze, H.Y., Yang, J.: Failure modes of sand in undrained cyclic loading: Impact of sample preparation. J. Geotech. Geoenviron. Eng. ASCE **140**(1), 152–169 (2014)
16. Triantafyllidis, Th. (ed.): Cyclic Behavior of Soils and Liquefaction Phenomena: Proceedings of the International Conference, Bochum, Germany. CRC Press (2004)
17. Vaid, Y.P., Stedman, J.D., Sivathayalan, S.: Confining stress and static shear effects in cyclic liquefaction. Can. Geotech. J. **38**(3), 580–591 (2001)
18. Wei, L.M., Yang, J.: On the role of grain shape in static liquefaction of sand-fines mixtures. Géotechnique **64**(9), 740–745 (2014)
19. Wei, X., Yang, J.: Cyclic behavior and liquefaction resistance of silty sands with presence of initial static shear stress. Soil Dyn. Earthq. Eng. (2018). https://doi.org/10.1016/j.soildyn.2018.11.029
20. Wichtmann, T., Hernandez, M., Triantafylidis, T.: On the influence of a non-cohesive fines content on small strain stiffness, modulus degradation and damping of quartz sand. Soil Dyn. Earthq. Eng. **69**, 103–114 (2015)
21. Yang, J.: Non-uniqueness of flow liquefaction line for loose sand. Géotechnique **52**(10), 757–760 (2002)
22. Yang, J., Gu, X.Q.: Shear stiffness of granular material at small strains: does it depend on grain size? Géotechnique **63**(2), 165–179 (2013)

23. Yang, J., Li, X.S.: State-dependent strength of sands from the perspective of unified modeling. J. Geotech. Geoenviron. Eng. ASCE **130**(2), 186–198 (2004)
24. Yang, J., Liu, X.: Shear wave velocity and stiffness of sand: the role of non-plastic fines. Géotechnique **66**(6), 500–514 (2016)
25. Yang, J., Liu, X., Guo, Y., Liang, L.B.: A unified framework for evaluating in situ state of sand. Géotechnique **68**(2), 177–183 (2018)
26. Yang, J., Sze, H.Y.: Cyclic behaviour and resistance of saturated sand under non-symmetrical loading conditions. Géotechnique **61**(1), 59–73 (2011)
27. Yang, J., Sze, H.Y.: Cyclic strength of sand under sustained shear stress. J. Gotech. Geoenviron. Eng. ASCE **137**(12), 1275–1285 (2011)
28. Yang, J., Wei, L.M.: Collapse of loose sand with the addition of fines: the role of particle shape. Géotechnique **62**(12), 1111–1125 (2012)
29. Yang, J., Wei, L.M., Dai, B.B.: State variables for silty sands: global void ratio or skeleton void ratio? Soils Founds **55**(1), 99–111 (2015)
30. Youd, T.L., Idriss, I.M., Andrus, R.D., Castro, G., Christian, J.T., Dobry, R., Finn, W.D.L., Harder Jr., L.F., Hynes, M.E., Ishihara, K., Koester, J.P., Liao, S.S.C., Marcuson III, W.F., Martin, G.R., Mitchell, J.K., Moriwaki, Y., Power, M.S., Robertson, P.K., Seed, R.B., Stokoe II, K.H.: Liquefaction resistance of soils: summary report from the 1996 NCEER and 1998 NCEER/NSF workshops on evaluation of liquefaction resistance of soils. J. Geotech. Geoenviron. Eng. ASCE **127**(10), 817–833 (2001)